International Journal of Advanced Structural Engineering, Vol. 3, No. 1, Pages 57-83, July 2011

Published online July 2011 at (http://journals.azad.ac.ir/IJASE)

IMPLEMENTATION OF HIGHER ORDER SHEAR THEORY ON ISOTROPIC MATERIAL AND LIU'S BENDING PART ON LAMINATED COMPOSITE FLAT SHELL ELEMENTS

Taufiq Rochman[1], Agoes Soehardjono[2] and Achfas Zacoeb[2]
Department of Civil Engineering, Brawijaya University, Malang, Indonesia

Received 15 April 2011
Revised 18 June 2011
Accepted 25 June 2011

Plate and shell analysis using classical plate theory (CPT) has a lack of accuracy in predicting the influence of transverse deformation, because of its assumption that the line normal to the surface remains straight and normal to the midplane before and after deformation. The next revision by constant shear deformation theory or famous as first order shear deformation theory (CSDT/FOSDT) still suffers a disadvantage that has a constant value in the shear term that is called shear locking phenomenon. This matter has been corrected by higher order shear deformation theory (HOSDT) using a refined assumption that the line normal to the surface should be in a parabolic function and not normal to the midplane, but normal to the surfaces so that it fulfills the zero strain in the surface. The analysis of the bending part of laminated composite flat shell element is applied by higher order lamination theory (HOLT) that is adopted from HOSDT. This model is accurate for thicknesses variation and complex materials. HOLT model is implemented into finite element procedure to find deflection, stresses and internal forces. It can be concluded that the displacement and stresses in HOLT model are higher than FOLT the ones (first order lamination theory) in small ratio of a/h dan its result almost the same value for a/h ratio more than 10. In a square plate case, the displacement gets smaller if the fiber arranged into cross-ply sequence. Interlaminar stresses along the thickness is not distributed continuously, but they have certain modes that depend on the depth of point position, the lamina or layer number, fiber orthotropic angle of each layer and a/h ratio.

Keywords: shear deformation; HOLT; laminated composite material, isotropic

[1] Ph.D. Student
[2] Professor

Correspondence to: Taufiq Rochman, Department of Civil Engineering, Brawijaya University, Malang, Indonesia, E-mail: taufiqrochman@gmail.com

1. Introduction

There are several models of plate and shell analysis. The first model is presented by Kirchoff and Love (1888) that is called classical plate theory (CPT). Actually CPT model is still adequate for very thin plate with the homogeneous and isotropic material. But for thicker plates and shells, this model has a serious shear problem that arises from its assumption that the line normal to the surface remains straight and normal to the midplane before and after deformation. Hence, CPT model neglected the transverse shear deformation that affected zero shear stress and strain in *xz* dan *yz* plane.

Then this theory was improved by Reissner and Mindlin (1951) with the next model that is known as constant shear deformation theory or first order shear deformation theory (CSDT/ FOSDT). This model is based on the assumption that the line normal to the surface remains straight but necessarily normal to the midplane after deformation. This model has already considered shear deformation only in a constant term, and this could make what is called shear locking phenomenon. They also did not meet the zero shear strain requirement at the surface.

Levinson (1980) corrected this problem by a refined assumption that the line normal to the surface should be in a parabolic function of the depth *z* and not normal to the midplane, but normal to the surface so that it fulfills the zero strain in the surfaces. This model is called higher order shear deformation theory (HOSDT). This model has a higher accuracy for both thin and thick plates and shells, homogeneous isotropic material or layered anisotropic ones.

Based on these problems, it can be described that the work objective is to find the deflection and stresses of laminated composite plates in certain plies configuration in FOLT (first order lamination theory) and HOLT model.

In order to make simplification, several conditions and basic assumptions are given: (1) The element is based on rectangular plate using HOLT model; (2) The properties of lamina is homogeneuous, elastic linear and tranversely isotropic with fiber angle and number of lamina variation; (3) Simple pinned boundary condition is used; (4) Dynamic and temperature is not considered in this analysis; (5) Normal stress in z direction is ignored ($\sigma_{zz} = 0$); (6) Bonding among lamina is assumed strong enough to hold any delamination.

2. Literature Review

2.1. One Way Composite Material

One way composite material consists of one-way fibers material as reinforcement that glued together in a matrix material. The direction of one way composites material that is called lamina is shown in Figure 1. Figure 2 shows one way bending and stress in the shell element.

In three dimensional element, stresses that occur in 6 face continuum cubic can be described by 6 stress components, 3 normal stresses σ_x, σ_y, σ_z, and 3 shear stresses $\tau_{xy}=\tau_{yx}$, $\tau_{xz}=\tau_{zx}$, $\tau_{yz}=\tau_{zy}$. All these stresses called three dimensional stresses.

Figure 3 shows structural global tensor and material local stress if they have the same global and local axes.

Considering fiber direction, unidirectional composite material is transversely isotropic material that has the same elastic component constants in 2 and 3 directions, because two perpendicular simetry planes have the same elastic constants.

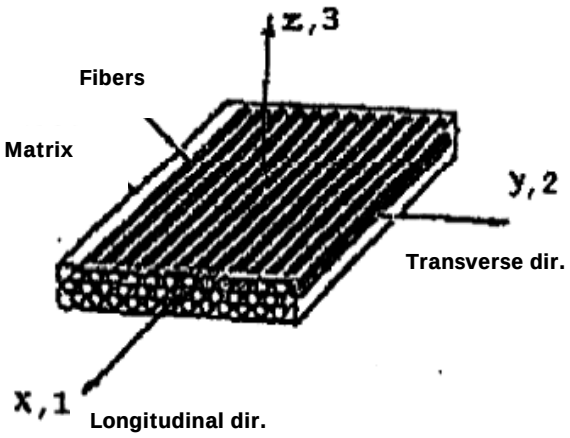

Figure 1. Lamina scheme (Hull, 1981)

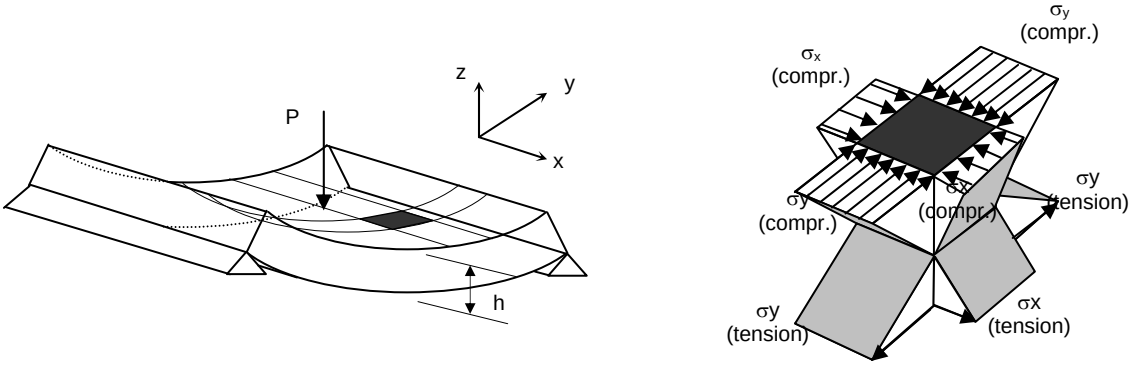

Figure 2. One way bending and stress in the shell element (*y* dominant bending direction)

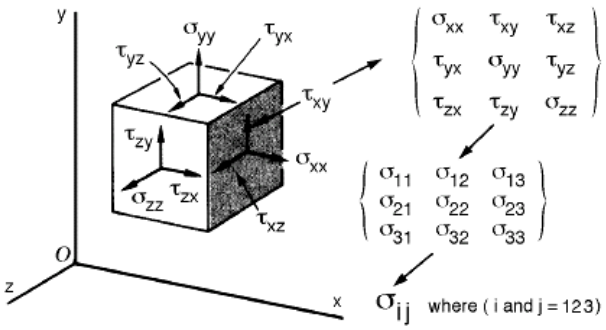

Figure 3. Continuum stress tensor (Kriz, 2000)

The relationship between stress and strain for transversely isotropic material hence can be shown as:

$$\{\sigma\}=[Q_{ij}].\{\varepsilon\} \qquad \text{or} \qquad \begin{Bmatrix}\sigma_1\\ \sigma_2\\ \tau_{23}\\ \tau_{13}\\ \tau_{12}\end{Bmatrix}=\begin{bmatrix}\frac{E_1}{1-\nu_{12}.\nu_{21}} & \frac{E_1.\nu_{21}}{1-\nu_{12}.\nu_{21}} & 0 & 0 & 0\\ \frac{E_1.\nu_{21}}{1-\nu_{12}.\nu_{21}} & \frac{E_2}{1-\nu_{12}.\nu_{21}} & 0 & 0 & 0\\ 0 & 0 & \frac{E_2}{2.(1+\nu_{23})} & 0 & 0\\ 0 & 0 & 0 & G_{12} & 0\\ 0 & 0 & 0 & 0 & G_{12}\end{bmatrix}.\begin{Bmatrix}\varepsilon_1\\ \varepsilon_2\\ \gamma_{23}\\ \gamma_{13}\\ \gamma_{12}\end{Bmatrix} \tag{1}$$

Fiber orthotropic angle β to the x and y axis shown in Figure 4. The local axis stress for β angle to the global axis is found by transforming structural global stress and strain component, $\{\sigma_s\}$ and $\{\varepsilon_s\}$ to the material local stress and strain, $\{\sigma_m\}$ and $\{\varepsilon_m\}$ as:

$$\{\sigma_m\}=\ \}=[T_\sigma].\{\sigma_s\ \} \quad \{\varepsilon_m\}=\{\varepsilon_m\}=[T_\varepsilon].\{\varepsilon_s\ \}$$

$$\begin{Bmatrix}\sigma_1\\ \sigma_2\\ \tau_{23}\\ \tau_{13}\\ \tau_{12}\end{Bmatrix}=[T_\sigma]\begin{Bmatrix}\sigma_x\\ \sigma_y\\ \tau_{yz}\\ \tau_{xz}\\ \tau_{xy}\end{Bmatrix} \qquad \begin{Bmatrix}\varepsilon_1\\ \varepsilon_2\\ \gamma_{23}\\ \gamma_{13}\\ \gamma_{12}\end{Bmatrix}=[T_\varepsilon]\begin{Bmatrix}\varepsilon_x\\ \varepsilon_y\\ \gamma_{yz}\\ \gamma_{xz}\\ \gamma_{xy}\end{Bmatrix} \tag{2}$$

where:

$$[T_\sigma]=\begin{bmatrix}c^2 & s^2 & 0 & 0 & 2cs\\ s^2 & c^2 & 0 & 0 & -2cs\\ -cs & cs & c & -s & 0\\ 0 & 0 & s & c & 0\\ -cs & cs & 0 & 0 & c^2-s^2\end{bmatrix} \quad [T_\varepsilon]=\begin{bmatrix}c^2 & s^2 & 0 & 0 & cs\\ s^2 & c^2 & 0 & 0 & -cs\\ -cs & cs & c & -s & 0\\ 0 & 0 & s & c & 0\\ -2cs & 2cs & 0 & 0 & c^2-s^2\end{bmatrix} \tag{3}$$

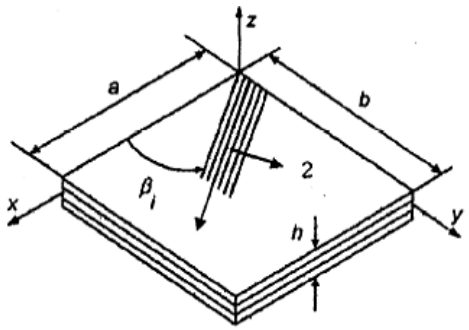

Figure 4. Fiber angle β in composite flat shell element (Rikard, 2000)

where: $c = \cos\beta$ and $s = \sin\beta$. The structural stress is shown below:

$$\begin{Bmatrix}\sigma_x\\ \sigma_y\\ \tau_{yz}\\ \tau_{xz}\\ \tau_{xy}\end{Bmatrix} = [T_\sigma]^{-1}.\begin{Bmatrix}\sigma_1\\ \sigma_2\\ \tau_{23}\\ \tau_{13}\\ \tau_{12}\end{Bmatrix} = [T_\sigma]^{-1}.[Q].\begin{Bmatrix}\varepsilon_1\\ \varepsilon_2\\ \gamma_{23}\\ \gamma_{13}\\ \gamma_{12}\end{Bmatrix} = [T_\sigma]^{-1}.[Q].[T_\varepsilon].\begin{Bmatrix}\varepsilon_x\\ \varepsilon_y\\ \gamma_{yz}\\ \gamma_{xz}\\ \gamma_{xy}\end{Bmatrix} \tag{4}$$

$$\begin{Bmatrix}\sigma_x\\ \sigma_y\\ \tau_{yz}\\ \tau_{xz}\\ \tau_{xy}\end{Bmatrix} = [\overline{Q}].\begin{Bmatrix}\varepsilon_x\\ \varepsilon_y\\ \gamma_{yz}\\ \gamma_{xz}\\ \gamma_{xy}\end{Bmatrix} \tag{5}$$

where:

$[\overline{Q}]$ = transformed reduced stiffness matrix:

$$[\overline{Q}] = \begin{bmatrix} \overline{Q}_{11} & \overline{Q}_{12} & 0 & 0 & \overline{Q}_{16} \\ \overline{Q}_{21} & \overline{Q}_{22} & 0 & 0 & \overline{Q}_{26} \\ 0 & 0 & \overline{Q}_{44} & \overline{Q}_{45} & 0 \\ 0 & 0 & \overline{Q}_{54} & \overline{Q}_{55} & 0 \\ \overline{Q}_{16} & \overline{Q}_{26} & 0 & 0 & \overline{Q}_{66} \end{bmatrix} \tag{6}$$

2.2. Lamination Analysis

2.2.1. General

Major constituents in a fiber-reinforced composite plates and shells are formed by the reinforcing fibers and a matrix, which acts as a binder for the fibers. The strength of a composite material

depends on the fiber strength and the matrix strength of the chemical bonds which holds them together. Usually composite plates and shells are arranged by several stacks of lamina called laminates that have certain orthotropic fiber angles. A microscopic zoom in μm scale of a cross-ply layered composite shown in Figure 5. Figure 6 shows the cross-ply arrangement of woven laminated composite and non-woven one.

2.2.2. Composite Act Assumption

In a composite plates or shells, it is assumed that every lamina has a full matrix interaction each other. Hence, they act as a non-homogen dan anisotropis laminates. This means that the bonds between two adjacent lamina surfaces are assumed strong enough to hold the shear stress so the displacement and or the strain through the thickness are assumed to be distributed continuously.

2.3. Classical Lamination Theory

Classical Lamination Theory (CLT) ignores transverse shear deformation in *xz* and *yz* plane that occurs between lamina. The lamina strain of CLT model is described as:

$$\begin{Bmatrix} \varepsilon_x \\ \varepsilon_y \\ \varepsilon_{xy} \end{Bmatrix} = \begin{Bmatrix} \varepsilon_x^0 \\ \varepsilon_y^0 \\ \varepsilon_{xy}^0 \end{Bmatrix} + z. \begin{Bmatrix} K_x \\ K_y \\ K_{xy} \end{Bmatrix} \tag{7}$$

Figure 7 shows the element laminates where n is the number of lamina and h_k is the related lamina thickness k^{th} and h_{k-1} is the previous lamina thickness *(k-1)*.

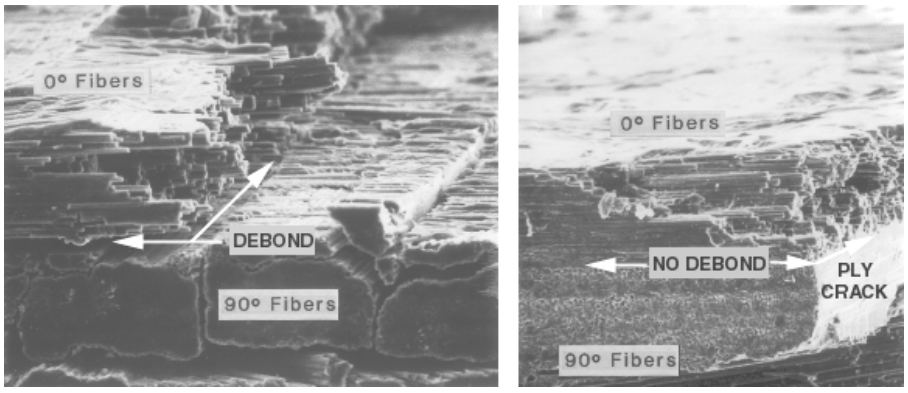

Figure 5. Fiber angle of laminated composite 0° and 90° in μm (Kriz, 2000)

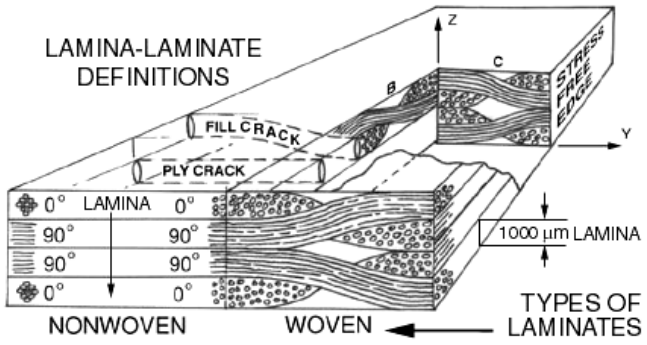

Figure 6. Fiber orientation in woven laminated composite (Kriz, 2000)

2.4. Plates and Shells: Theory and Development

Figures 7 and 8 show overall deformation, total strain and laminate nomenclature used in ABD matrix, respectively. Plates and shells element internal forces such as moment M_x, M_y, M_{xy} and shear forces Q_x and Q_y and normal forces N_x, N_y and N_{xy} are shown in Figure 9.

CPT model rotation can be formulated as:

$$\frac{dw}{dx} = -\psi_x \; ; \qquad \frac{dw}{dy} = \psi_y \tag{8}$$

And the displacement field of CPT model in the *x*, *y*, and *z* direction is:

$$u = -z\frac{dw}{dx} \; ; \; v = -z\frac{dw}{dy} \; ; \; w = w(x,y) \tag{9}$$

The total rotation of FOSDT model is:

$$\gamma_{zx} = \frac{dw}{dx} - \psi_x \; ; \; \gamma_{zy} = \frac{dw}{dx} - \psi_y \tag{10}$$

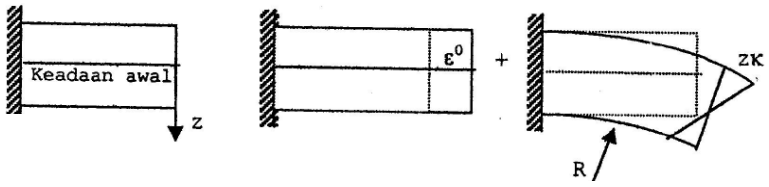

Figure 7. Total strain (Matthews, 1991)

Figure 8. Laminate nomenclature used in ABD matrix (Hyer, 1998)

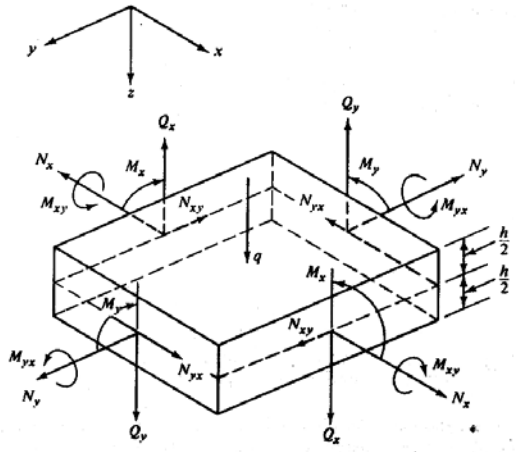

Figure 9. Internal forces direction in the *x*, *y*, *z* axis (Szilard, 1974)

While the FOSDT model displacement field can be described in *x*, *y* and *z* direction as:

$$u = -z.\psi_x \;;\; v = -z.\psi_y \;;\; w = w(x,y) \tag{11}$$

Otherwise, the third model, HOSDT, is based on the assumption that the deformed normal plane is in the parabolic line to approach an actual deformation. This model has shear transverse value and always fullfils the zero shear strain in the surfaces because the normal line perpendicular in both surfaces where the shell depth is $z = \pm h/2$. The displacement field of HOSDT model in the x, y, z direction follow:

$$\begin{aligned} u(x,y,z) &= u_o(x,y,z) + z.\psi_x(x,y,z) + z^3\phi_x(x,y,z) \\ v(x,y,z) &= v_o(x,y,z) + z.\psi_y(x,y,z) + z^3\phi_y(x,y,z) \\ w(x,y,z) &= w_o(x,y,z) \end{aligned} \tag{12}$$

The normal line assumption differences among three models for undeformed and deformed section are given in Figure 10. The displacement direction, rotation and their derivative of HOSDT plates and shells model are shown in Figure 11.

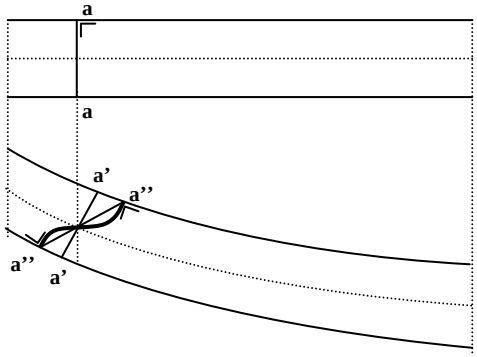

a-a = the undeformed normal line

a'-a' = the deformed CST's normal (Kirchoff-Love)

a''-a''= the deformed FOSDT's (Reissner-Mindlin) (straight line)

a''-a''= the deformed HOSDT's (Levinson-Reddy) (parabolic bold line)

Figure 10. The assumption differences of the shell normal line among three models (Levinson, 1980)

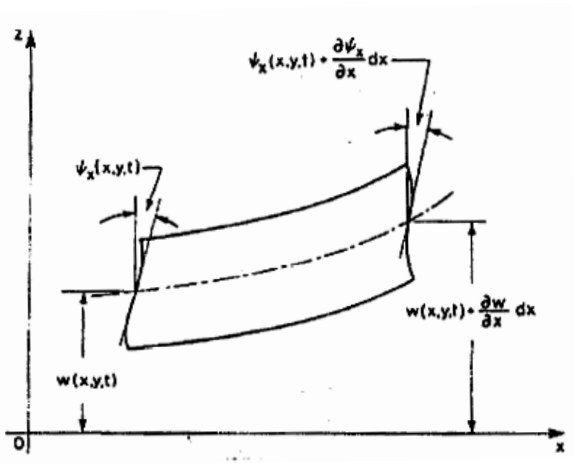

Figure 11. Displacement, rotation and their derivative (M. Levinson, 1980)

The strain ε and the shear rotation γ in the *xz* and *yz* plane are:

$$\varepsilon_{xz} = \frac{1}{2}\gamma_{xz} = \frac{1}{2}\left(\frac{\partial w}{\partial x} + \frac{\partial u}{\partial z}\right) \qquad \varepsilon_{yz} = \frac{1}{2}\gamma_{yz} = \frac{1}{2}\left(\frac{\partial w}{\partial y} + \frac{\partial v}{\partial z}\right) \tag{13}$$

Setting the zero shear strain γ_{xz} and γ_{yz} in the surfaces in Equation (13) for $z = \pm h/2$, the kinematic variable ϕ_x and ϕ_y computed as:

$$\phi_x = -\frac{4}{3h^2}\left(\psi_x + \frac{\partial w}{\partial x}\right) \qquad \phi_y = -\frac{4}{3h^2}\left(\psi_y + \frac{\partial w}{\partial y}\right) \tag{14}$$

Subsituting Equation (14) into Equations (12) and (13), results the strain $\{\varepsilon\}$ of HOSDT model:

$$\varepsilon_x = \frac{\partial u}{\partial x} = \frac{\partial u_{ox}}{\partial x} + z.\left(1 - \frac{4.z^2}{3h^2}\right)\frac{\partial \psi_x}{\partial x} - \frac{4.z^3}{3.h^2}.\frac{\partial^2 w}{\partial x^2}$$

$$\varepsilon_y = \frac{\partial v}{\partial y} = \frac{\partial v_{oy}}{\partial y} + z.\left(1 - \frac{4.z^2}{3h^2}\right)\frac{\partial \psi_y}{\partial y} - \frac{4.z^3}{3.h^2}.\frac{\partial^2 w}{\partial y^2}$$

$$\gamma_{xy} = \frac{\partial u}{\partial y} + \frac{\partial v}{\partial x} = \frac{\partial u_{ox}}{\partial y} + \frac{\partial v_{oy}}{\partial x} + z.\left(1 - \frac{4.z^2}{3h^2}\right).\left(\frac{\partial \psi_x}{\partial y} + \frac{\partial \psi_y}{\partial x}\right) - \frac{8.z^3}{3.h^2}\frac{\partial^2 w}{\partial x \partial y}$$

$$\gamma_{xz} = \frac{\partial w}{\partial x} + \frac{\partial u}{\partial z} = z.\left(1 - \frac{4.z^2}{h^2}\right).\left(\psi_x + \frac{\partial w}{\partial x}\right)$$

$$\gamma_{yz} = \frac{\partial w}{\partial y} + \frac{\partial v}{\partial z} = z.\left(1 - \frac{4.z^2}{h^2}\right).\left(\psi_x + \frac{\partial w}{\partial y}\right) \tag{15}$$

Then the stress $\{\sigma\}$ of this model is found from strain $\{\varepsilon\}$ in Equation (15) become:

$$\sigma_x = \frac{E}{1-\nu^2}\left(\varepsilon_x + \nu.\varepsilon_y\right)$$

$$= \frac{E}{1-\nu^2}\left[f_1(z).\left(\frac{\partial \psi_x}{\partial x} + \nu.\frac{\partial \psi_y}{\partial y}\right) - f_2(z).\left(\frac{\partial^2 w}{\partial x^2} + \nu.\frac{\partial^2 w}{\partial y^2}\right)\right]$$

$$\sigma_y = \frac{E}{1-\nu^2}\left(\nu.\varepsilon_x + \varepsilon_y\right)$$

$$= \frac{E}{1-\nu^2}\left[f_1(z).\left(\nu.\frac{\partial \psi_x}{\partial x} + \frac{\partial \psi_y}{\partial y}\right) - f_2(z).\left(\nu.\frac{\partial^2 w}{\partial x^2} + \frac{\partial^2 w}{\partial y^2}\right)\right]$$

$$\tau_{xy} = 2.G.\varepsilon_{xy} = G.\gamma_{xy}$$

$$= G.\left[f_1(z).\left(\frac{\partial \psi_x}{\partial y} + \frac{\partial \psi_y}{\partial x}\right) - 2.f_2(z)\frac{\partial^2 w}{\partial x \partial y}\right]$$

$$\tau_{xz} = 2.G.\varepsilon_{xz} = G.\gamma_{xz}$$

$$= G.\left[f_3(z).\psi_x + f_4(z)\frac{\partial w}{\partial x}\right]$$

$$\tau_{yz} = 2.G.\varepsilon_{yz} = G.\gamma_{yz}$$

$$= G.\left[f_3(z).\psi_y + f_4(z)\frac{\partial w}{\partial y}\right] \qquad (16)$$

where: $G = \frac{E}{2.(1+\nu)}$

$$f_1(z) = z.\left(1 - \frac{4.z^2}{3.h^2}\right)$$

$$f_2(z) = \frac{4.z^3}{3.h^2}$$

$$f_3(z) = z.\left(1 - \frac{4.z^2}{h^2}\right)$$

$$f_4(z) = \left(1 - \frac{4.z^2}{h^2}\right)$$

Finally, the internal forces *M*, *N* and *Q* HOSDT model described as:

$$M_x = \int_{-\frac{h}{2}}^{\frac{h}{2}} \sigma_x.z \; dz = \frac{1}{5}.D\left(\frac{\partial^2 w}{\partial x^2} + \nu.\frac{\partial^2 w}{\partial y^2}\right) + \frac{4}{5}.\left(1 + \tfrac{1}{h}\right).D.\left(\frac{\partial \psi_x}{\partial x} + \nu\frac{\partial \psi_y}{\partial y}\right) \qquad (17)$$

$$M_y = \int_{-\frac{h}{2}}^{\frac{h}{2}} \sigma_y .z \; dz = \frac{1}{5}.D\left(\nu.\frac{\partial^2 w}{\partial x^2} + \frac{\partial^2 w}{\partial y^2}\right) + \frac{4}{5}.\left(1+\tfrac{1}{h}\right).D.\left(\nu.\frac{\partial \psi_x}{\partial x} + \frac{\partial \psi_y}{\partial y}\right)$$

$$M_{xy} = \int_{-\frac{h}{2}}^{\frac{h}{2}} \tau_{xy} .z \; dz = \frac{1}{5}.D.(1-\nu).\left[2.\left(1+\tfrac{1}{h}\right).\left(\frac{\partial \psi_x}{\partial y} + \frac{\partial \psi_y}{\partial x}\right) - \frac{\partial^2 w}{\partial x \partial y}\right]$$

$$N_x = \int_{-\frac{h}{2}}^{\frac{h}{2}} \sigma_x \, dz = \frac{1}{2.h} D.\left[5.\left(\frac{\partial \psi_x}{\partial x} + \nu.\frac{\partial \psi_y}{\partial y}\right) - \left(\frac{\partial^2 w}{\partial x^2} + \nu.\frac{\partial^2 w}{\partial y^2}\right)\right]$$

$$N_y = \int_{-\frac{h}{2}}^{\frac{h}{2}} \sigma_y \, dz = \frac{1}{2.h} D.\left[5.\left(\nu.\frac{\partial \psi_x}{\partial x} + \frac{\partial \psi_y}{\partial y}\right) - \left(\nu.\frac{\partial^2 w}{\partial x^2} + \frac{\partial^2 w}{\partial y^2}\right)\right]$$

$$N_x = \int_{-\frac{h}{2}}^{\frac{h}{2}} \sigma_x dz = \frac{5}{2h} D(1+v)\left[\left(\frac{\partial \psi_x}{\partial x} + \frac{\partial \psi_y}{\partial y}\right) - \frac{1}{5}\left(\frac{\partial^2 w}{\partial x^2} + \frac{\partial^2 w}{\partial y^2}\right)\right]$$

$$N_x = \int_{-\frac{h}{2}}^{\frac{h}{2}} \sigma_y dz = \frac{5}{2h} D(1+v)\left[\left(\frac{\partial \psi_x}{\partial x} + \frac{\partial \psi_y}{\partial y}\right) - \frac{1}{5}\left(\frac{\partial^2 w}{\partial x^2} + \frac{\partial^2 w}{\partial y^2}\right)\right] \qquad (18)$$

$$N_{xy} = \int_{-\frac{h}{2}}^{\frac{h}{2}} \tau_{xy} dz = \frac{5}{4h} D(1+v)\left[\left(\frac{\partial \psi_x}{\partial x} + \frac{\partial \psi_y}{\partial y}\right) - \frac{8}{5}\left(\frac{\partial^2 w}{\partial x^2} + \frac{\partial^2 w}{\partial y^2}\right)\right]$$

$$Q_x = \int_{-\frac{h}{2}}^{\frac{h}{2}} \tau_{xz} dz = \frac{2}{3} Gh.\left(\psi_x + \frac{\partial w}{\partial x}\right)$$

$$Q_y = \int_{-\frac{h}{2}}^{\frac{h}{2}} \tau_{yz} dz = \frac{2}{3} Gh.\left(\psi_y + \frac{\partial w}{\partial y}\right) \qquad (19)$$

2.5. Laminated Composite Analysis (HOLT)

Analysis of HOSDT model for laminated case is called HOLT (*Higher Order Lamination Theory*). There are shear stress component of γ_{xz} and γ_{yz} should be added into ABD matrix as an important modification. Hence, below are the internal forces of HOLT model:

$$\begin{bmatrix} N_x \\ N_y \\ N_{xy} \\ M_x \\ M_y \\ M_{xy} \\ P_x \\ P_y \\ P_{xy} \\ Q_y \\ Q_x \end{bmatrix} = \begin{bmatrix} A_{11} & A_{12} & A_{16} & B_{11} & B_{12} & B_{16} & E_{11} & E_{12} & E_{16} & 0 & 0 \\ & A_{22} & A_{26} & B_{12} & B_{22} & B_{26} & E_{12} & E_{22} & E_{26} & 0 & 0 \\ & & A_{66} & B_{16} & B_{26} & B_{66} & E_{16} & E_{26} & E_{66} & 0 & 0 \\ & & & D_{11} & D_{12} & D_{16} & F_{11} & F_{12} & F_{16} & 0 & 0 \\ & & & & D_{22} & D_{26} & F_{12} & F_{22} & F_{26} & 0 & 0 \\ & & & & & D_{66} & F_{16} & F_{26} & F_{66} & 0 & 0 \\ & & & & & & H_{11} & H_{12} & H_{16} & 0 & 0 \\ & & & & & & & H_{22} & H_{26} & 0 & 0 \\ & & & & & & & & H_{66} & 0 & 0 \\ & & & & & & & & & S_{44} & S_{45} \\ & & & & & & & & & & S_{55} \end{bmatrix} \cdot \begin{bmatrix} \varepsilon_{x0} \\ \varepsilon_{y0} \\ \gamma_{xy0} \\ \frac{\partial \varphi_x}{\partial x} \\ \frac{\partial \varphi_y}{\partial y} \\ \left(\frac{\partial \varphi_x}{\partial y} + \frac{\partial \varphi_y}{\partial x}\right) \\ \frac{\partial^2 w}{\partial x^2} \\ \frac{\partial^2 w}{\partial y^2} \\ 2\frac{\partial^2 w}{\partial x \partial y} \\ \varphi_y \\ \varphi_x \end{bmatrix} \tag{20}$$

where:

$$\begin{aligned} \left(A_{ij}, B_{ij}, D_{ij}, E_{ij}, F_{ij}, H_{ij}\right) &= \int_{-\frac{h}{2}}^{\frac{h}{2}} \left(1, z, z^2, -\tfrac{4}{3h^2} z^3, -\tfrac{4}{3h^2} z^4, z^6\right) \overline{Q}_{ij} \\ S_{kl} &= \int_{-\frac{h}{2}}^{\frac{h}{2}} f'(z)\ \overline{Q}_{kl}\, dz = \int_{-\frac{h}{2}}^{\frac{h}{2}} \left(1 - \tfrac{4z^2}{3h^2}\right) \overline{Q}_{kl} \end{aligned} \tag{21}$$

where i, j = 1,2,6 and k, l = 4, 5.

The E_{ij}, F_{ij}, H_{ij} and S_{ij} coefficient is higher order normal component, moment and shear respectively. The integration through the plates or shell thicknesses are modified for lamina homogenization objective, then results ABDEFH components as:

$$\begin{aligned} A_{ij} &= \sum_{k=1}^{n} \overline{Q}_{ij}^{(k)} \left(h_k - h_{k-1}\right) & E_{ij} &= -\frac{1}{3h^2} \sum_{k=1}^{n} \overline{Q}_{ij}^{(k)} \left(h_k^{\,4} - h_{k-1}^{\,4}\right) \\ B_{ij} &= \frac{1}{2} \sum_{k=1}^{n} \overline{Q}_{ij}^{(k)} \left(h_k^{\,2} - h_{k-1}^{\,2}\right) & F_{ij} &= -\frac{4}{15h^2} \sum_{k=1}^{n} \overline{Q}_{ij}^{(k)} \left(h_k^{\,5} - h_{k-1}^{\,5}\right) \\ D_{ij} &= \frac{1}{3} \sum_{k=1}^{n} \overline{Q}_{ij}^{(k)} \left(h_k^{\,3} - h_{k-1}^{\,3}\right) & H_{ij} &= \frac{1}{7} \sum_{k=1}^{n} \overline{Q}_{ij}^{(k)} \left(h_k^{\,7} - h_{k-1}^{\,7}\right) \\ S_{kl} &= \sum_{k=1}^{n} \overline{Q}_{kl}^{(k)} \left(\left(h_k - \frac{4h_k^{\,3}}{3h^2}\right) - \left(h_{k-1} - \frac{4h_{k-1}^{\,3}}{3h^2}\right)\right) \end{aligned} \tag{22}$$

3. Methodology

3.1. Problem Description

The assumptions in solving the bending part of HOLT shell element model for laminated composite material are the same with basic assumptions in the previous, except that several assumptions should be added:

1. Small deflection HOLT plate bending model, is used that have range $^1/_{10}\ h - {}^1/_5\ h$.
2. Rectangular plate bending element with 5 DOF is used.
3. Different shape function for displacement w and the rotation are used to avoid shear locking effect.

3.2. Bending Part FE Formulation

Each element has 4 nodals shown in Figure 12.

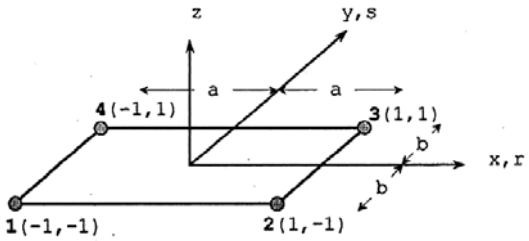

Figure 12. Plate bending scheme (Weaver, 1989)

Each nodal have 5 DOFs are w, $^{dw}/_{dx}$, $^{dw}/_{dy}$, φ_x and φ_y shown in Figure 13 below:

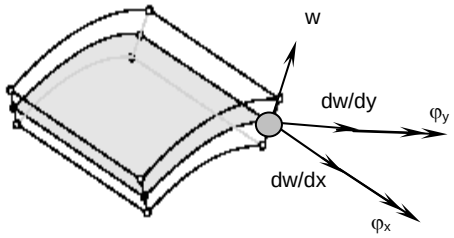

Figure 13. Degree of freedoms of HOLT plate bending element

The symbol of φ is defined as:

$$\varphi_x = \frac{\left(\frac{dw}{dx} + \psi_x\right)}{h^2} \qquad \varphi_y = \frac{\left(\frac{dw}{dy} + \psi_y\right)}{h^2} \tag{23}$$

3.2.1. Interpolation Function

In determining this section, we follow Liu's methodology for homogeneous case. Liu has formulated a good bending element, so that's why we use his element. But it should be made a little modification in stiffness matrix, because the convention in the material literatures does not meet FEM literatures have in the sequence of γ_{xz} and γ_{yz} terms. It will be called Liu modified element.

In order to make the reader easy and comfort in tracing the literature, it should be describe briefly in the following section. The displacement w used as an optimal interpolation function S_i, while two rotations in Equation (23) use bilinear Lagrange interpolation function, N_i:

$$w = \sum_{i=1}^{12} S_i \, \delta_i \qquad \varphi_x = \sum_{i=1}^{4} N_i \, \varphi_{xi} \qquad \varphi_y = \sum_{i=1}^{4} N_i \, \varphi_{yi} \tag{24}$$

Equation (24) results $\{\bar{w}\}_{3x1}$ by multiplying $[\bar{N}]_{3x20}$ matrix with $\{\bar{\delta}\}_{20x1}$ vector:

$$\{\bar{w}\} = [\bar{N}]\{\bar{\delta}\} \tag{25}$$

where:

$$\{\bar{w}\} = \begin{Bmatrix} w \\ \varphi_x \\ \varphi_y \end{Bmatrix}$$

From the Equation (26) it can be seen that the displacement w used [S] shape function, because it needs higher derivation of w, so the displacement shape function should have higher order too.

$$[\bar{N}] = \begin{bmatrix} [S] & 0 & 0 & 0 & 0 & 0 & 0 & 0 & 0 \\ 0 & N_1 & 0 & N_2 & 0 & N_3 & 0 & N_4 & 0 \\ 0 & 0 & N_1 & 0 & N_2 & 0 & N_3 & 0 & N_4 \end{bmatrix}$$

$$\{\bar{\delta}\} = \{\delta_1 \quad \delta_2 \quad .... \quad \delta_{12} \quad \varphi_{x1} \quad \varphi_{y1} \quad \varphi_{x2} \quad \varphi_{y2} \quad \varphi_{x3} \quad \varphi_{y3} \quad \varphi_{x4} \quad \varphi_{y4}\} \tag{26}$$

$$N_1 = \frac{1}{4}.(1-r)(1-s) \qquad N_2 = \frac{1}{4}.(1+r)(1-s)$$

$$N_3 = \frac{1}{4}.(1+r)(1+s) \qquad N_4 = \frac{1}{4}.(1-r)(1+s)$$

$$[S]^T = \begin{bmatrix} f_1(r)h_1(s,t_2)+f_1(s)h_1(r,t_2)-h_1(s,t_2)h_1(r,t_2) \\ g(s)h_1(r,p)b_e \\ -g(r)h_1(s,q)a_e \\ f_1(1-r)h_1(s,t_2)+f_1(s)h_1(1-r,t_2)-h_1(s,t_2)h_1(1-r,t_2) \\ g(s)h_1(1-r,p)b_e \\ g(1-r)h_1(s,q)a_e \\ f_1(1-r)h_1(1-s,t_2)+f_1(1-s)h_1(1-r,t_2)-h_1(1-s,t_2)h_1(1-r,t_2) \\ -g(1-s)h_1(1-r,p)b_e \\ g(1-r)h_1(1-s,q)a_e \\ f_1(r)h_1(1-s,t_2)+f_1(1-s)h_1(r,t_2)-h_1(1-s,t_2)h_1(r,t_2) \\ -g(1-s)h_1(r,p)b_e \\ -g(r)h_1(1-s,q)a_e \end{bmatrix} \quad (27)$$

where r=x/a, s=y/b, while p, q and t_2 is the variable parameters determined from the convergence requirement. The best result is found if the value of p=q=1 and t_2=2. The f_1, g and h_1 function in Equation (27) can be defined as:

$$\begin{aligned} & f_1(t_1) = (1-t_1)^2(1+2t_1) \\ & g\left(t_1^{(3-6)}(1-t_1)^2\right) \\ & h_1(t_1,t_3) = (1-t_1)\left(1+\frac{t_1t_3}{2}-t_3t_1^2\right) \end{aligned} \quad (28)$$

where t_1 and t_3 is dependent variables.

Further detail of generalized strain vector $\{\varepsilon_g\}_{8x1}$, $[B]_{8x20}$ matrix and $\{\bar{\delta}\}_{20x1}$ displacement vector can be read in Liu's paper. Strain component of HOLT model, $\{\varepsilon\}_{5x1}$ is found by multiplying an operator matrix $[T(z)]_{5x8}$ by generalized strain vector $\{\varepsilon_g\}_{8x1.}$

$$\{\varepsilon\} = [T(z)]\{\varepsilon_g\} \quad (29)$$

T(z) is a displacement u, v, w shape function operator of HOSDT model. T(z) operator is:

$$[T(z)] = \begin{bmatrix} -z & 0 & 0 & f(z)h^2 & 0 & 0 & 0 & 0 \\ 0 & -z & 0 & 0 & f(z)h^2 & 0 & 0 & 0 \\ 0 & 0 & 0 & 0 & 0 & f'(z)h^2 & 0 & 0 \\ 0 & 0 & 0 & 0 & 0 & 0 & f'(z)h^2 & 0 \\ 0 & 0 & -z & 0 & 0 & 0 & 0 & f(z)h^2 \end{bmatrix} \quad (30)$$

where:

$f(z)=\left(1-\frac{4z^2}{3h^2}\right)$ and f'(z) is its derivative. The element stiffness matrix, $[k]_{20x20}$ is determined by multiplying $[B]^T_{20x8}$ matrix and $[D]_{8x8}$ matrix and then multiplied by the result with $[B]_{8x20}$ matrix.

$$[k]_e = \int [B]^T [D] [B] \, dx \, dy \tag{31}$$

Where $[D]_{8x8}$ is the homogenized material matrix found by multiplying $[T(z)]^T_{8x5}$ matrix with $\left[\overline{Q}\right]_{5x5}$ matrix and then multiplying the result by $[T(z)]_{5x8}$ matrix, and integrate the result through the lamina thicknesses. The $[D]_{8x8}$ matrix is found by sum the results above, hence:

$$[D]=\sum_{1}^{n}\int_{h_{k-1}}^{h_k}[T(z)]^T\left[\overline{Q}\right][T(z)]dz \tag{32}$$

Where n is lamina number, while h_{k-1} and h_k is the bottom and top coordinates at the k^{th} lamina respectively. Hence [D] in Equation (32) is the material homogenized matrix for laminated composite materials. Equation (31) can be solved by using 2x2 Gauss quadrature become:

$$[k]=|J|.h.\sum_{j=1}^{n}\sum_{i=1}^{n}W_iW_j\,[B(\pm 0.57735,\pm 0.57735)]^T[D][B(\pm 0.57735,\pm 0.57735)]$$

4. Results and Discussions

4.1. Benchmark Data

The calculation data used are of two types. First, isotropic material data for verification and validity between exact result by Timoshenko from linear elasticity theory and the HOSDT model, SAP90 software and also Stardyne thick and thin Element from STAADPro2000 software. Second, the laminated composite data follow Singh analysis, as a benchmark validation to compare the result of HOLT model, FOLT model and also the exact results from the elasticity theory.

4.1.1. Isotropic Data

Plate is simply supported in a square geometric a=b=1, plate thicknesses is varied from 0.25 through 0.01, Poisson ratio ν=0.25, and Young elastic modulus, E=1. There are three types of loading; sinusoidal load, distributed load and concentrated point load.

4.1.2. Laminated Composite Material Data

A symmetric laminate is arranged into four layers with the stack sequence of cross-ply fiber angle from top fiber respectively [0°/90°/90°/0°]. These example data use Pagano's analysis as an exact benchmark. The characteristic lamina material data is illustrated in Table 1.

Table 1. Characteristic lamina material data (Krishnamoorty, 1987)

E_1 (GPa)	E_2 (GPa)	ν_{12}	ν_{21}	G_{12} (GPa)	G_{13} (GPa)	G_{23} (GPa)
175	7	0.25	0.01	3.5	3.5	1.4

4.1.3. Plate Geometric Data

The plate geometric data will be observed as: (1) A square plate, where a/b=1; (2) The value of a/h ratio are 4, 5, 10, 20, 50 and 100 respectively; (3) The fiber angle is varied at intervals 0° to 90° (with 15° increments); (4) Simply supported condition at the entire edge of the plate; (5) The elements discretization is varied as 4, 9, 16 and 25 elements to check the convergence.

4.2. Analysis Results

4.2.1. Isotropic Case

The maximum deflection result, w_o of an isotropic plate is shown in Tables 2 to 4. At the ratio of a/h=4, the linear elasticity HOSDT model compared with Timoshenko, SAP90, Stardyne Thick Element and Stardyne Thin Element results differ as much as 24.68 %, 17.27 %, -20.08 % dan 26.76 % respectively. For sinusoidal loading, HOSDT model result lies between SAP90 and Stardyne-thick result from STAADPro2000 software at the small a/h ratio and almost the same with Timoshenko and Stardyne-thin results at the large ratio of a/h.

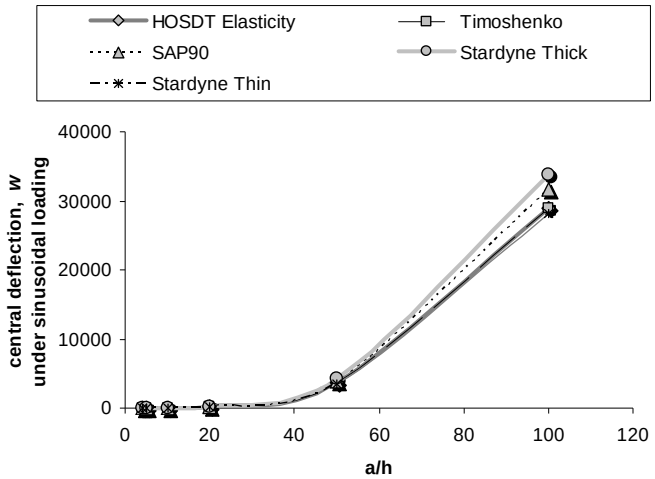

Figure 14. The central deflection w_o and a/h ratio relationship for sinusoidal loading

At the ratio of a/h=4, the differences of linear elasticity HOSDT model compared with Timoshenko, SAP90, Stardyne Thick Element and Stardyne Thin Element are 24.68 %, 26.47 %, -5.80 % dan 26.61 %, respectively.

For distributed loading, HOSDT model results lie between Stardyne-Thick and Timoshenko results at the small a/h ratio but approaching Timoshenko's result at the large ration of a/h.

At the ratio of a/h=4, the linear elasticity HOSDT model compared with Timoshenko, SAP90, Stardyne Thick Element and Stardyne Thin Element results differ as much as 17.76 %, 14.40 %, -67.96 % dan 15.20 %, respectively.

Table 2. The central deflection w_o (sinusoidal loading) in simply supported isotropic plate

a/h	HOSDT Elasticity	Timoshenko q. $a^4 / (4\pi^4 D)$	SAP90 (4x4)	Stardyne Thick (4x4)	Stardyne Thin (4x4)
4	2.45342	1.84787	2.0297	2.946	1.797
5	4.36715	3.60912	3.96425	5.238	3.510
10	30.3918	28.8729	31.7141	35.991	28.081
20	234.023	230.983	253.712	275.133	224.647
50	3616.72	3609.12	3964	4241.353	3510.111
100	28888.1	28873	31710	33864.47	28080.88

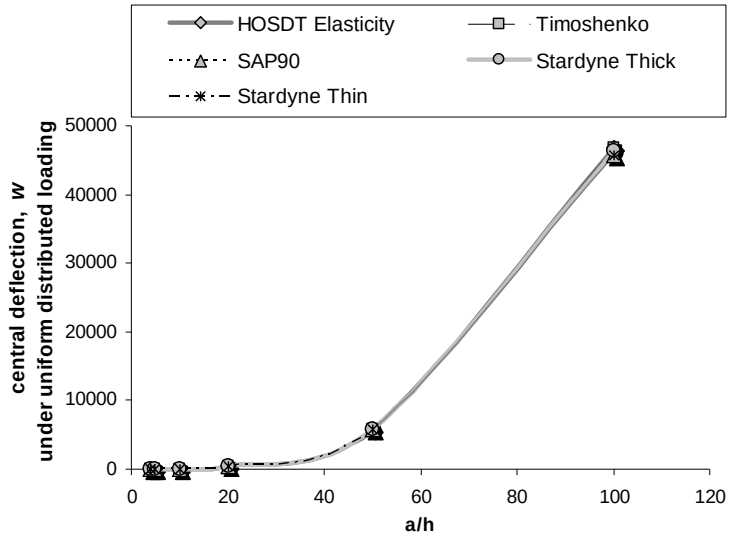

Figure 15. Central deflection w_o and a/h ratio relationship for distributed loading

Table 3. Central deflection w_o (distributed loading) in simply supported isotropic plates

a/h	HOSDT Elasticity	Timoshenko 4.q. $a^4/(4\pi^6 D)$	SAP90 (4x4)	Stardyne Thick (4x4)	Stardyne Thin (4x4)
4	3.97734	2.99566	2.92459	4.208	2.919
5	7.07973	5.8509	5.71211	7.511	5.702
10	49.2694	46.8071	45.6969	51.019	45.616
20	379.384	374.457	365.575	382.513	364.927
50	5863.21	5850.9	5712	5829.631	5701.977
100	46831.8	46807.2	45700	46445.99	45615.81

Tabel 4. Central deflection w_o (concentrated loading) in simply supported isotropic plate

a/h	HOSDT Elasticity	Timoshenko 4.q. $a^4/(4\pi^6 D)$	SAP90 (4x4)	Stardyne Thick (4x4)	Stardyne Thin (4x4)
4	9.81372	8.0712	8.400912	16.483	8.322
5	17.4685	15.764	16.40803	26.947	16.253
10	121.567	126.112	131.2642	156.276	130.025
20	936.094	1008.9	1019	1115.315	1040.197
50	14466.9	15764	16410	16760.63	16253.09
100	115552	126112	131300	133270	130020

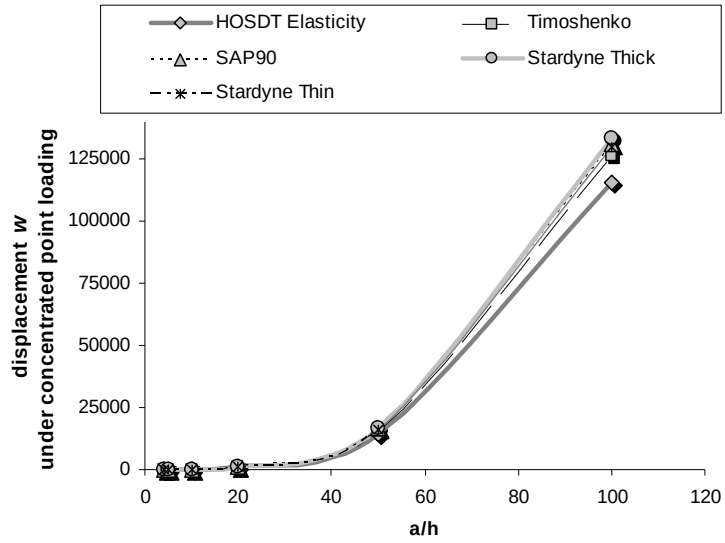

Figure 16. Central deflection w_o and a/h ratio relationship for concentrated loading

For concentrated loading, HOSDT model results are larger than SAP90 at ratio of a/h=4 and a/h=5, but they are smaller than all the models at a/h ratio between range 10 and 100.

4.2.2. Laminated Composite Case

As for the laminated composite plate the results shown in Table 5 below:

Table 5. Non-dimensional central deflection w and stress σ in laminated composite plate $[0^o/90^o]_S$,

a/h	Analysis	w*	σ_1^*	σ_2^*	τ_{23}^*	τ_{13}^*	τ_{12}^*
	Exact	1.9540	0.7200	-	0.2920	0.2190	0.0467
4	HOLT	1.9029	0.7123	0.0715	0.2244	0.2137	0.0463
	FOLT	1.7100	0.4059	0.0689	0.1963	0.1398	0.0308
	Exact	1.4685	-	-	-	-	-
5	HOLT	1.4235	0.6924	0.0597	0.1899	0.2460	0.0304
	FOLT	-	-	-	-	-	-
	Exact	0.7434	0.5990	-	0.1960	0.3010	0.0276
10	HOLT	0.7147	0.5523	0.0371	0.2243	0.2492	0.0268
	FOLT	0.6628	0.4989	-	0.1292	0.1667	0.0241
	Exact	0.5173	0.5430	-	0.1560	0.3280	0.0230
20	HOLT	0.5071	0.5406	0.0326	0.1933	0.2639	0.0228
	FOLT	0.4912	0.5273	-	0.1087	0.1749	0.0221
	Exact	0.4446	-	-	-	-	-
50	HOLT	0.4434	0.5281	0.0168	0.1175	0.2735	0.0216
	FOLT	-	-	-	-	-	-
	Exact	0.4385	0.5390	-	0.1380	0.3390	0.0213
100	HOLT	0.4343	0.5239	0.0087	0.1174	0.2883	0.0246
	FOLT	-	-	-	-	-	-

The meaning of w* and σ* in the Table 5 are the non-dimensional deflection and stresses:

$$
\begin{aligned}
W^*\tau_{12}^* &= \tau_{12}\ (0,0,+\frac{h}{2})\frac{h^2}{q\circ a^2} \\
\sigma_1^* &= \sigma_1(\frac{a}{2},\frac{b}{2},+\frac{h}{2})\frac{h^2}{q\circ a^2} \\
\sigma_2^* &= \sigma_2(\frac{a}{2},\frac{b}{2},+\frac{h}{2})\frac{h^2}{q\circ a^2} \\
\tau_{23}^* &= \tau_{23}(\frac{n}{2},0,0)\frac{h}{q\circ a} \\
\tau_{13}^* &= \tau_{13}(0,\frac{b}{2},0)\frac{h}{q\circ a}
\end{aligned}
\qquad (33)
$$

$$\tau_{12}^{*} = \tau_{12}\left(0,0,+\frac{h}{2}\right)\frac{h^2}{q_o a^2}$$

The meaning of $w(^{a}/_{2},^{b}/_{2})$ is the maximum deflection w_o at the plate center x=a/2 and y=b/2. While $\tau_{12}(0,0,+^{h}/_{2})$ is shear stress in the plane 1-2 at plate edge where x=0 and y=0 and the plate top surface $z=+^{h}/_{2}$.

4.3. Parametric Study

In the discussion will be shown the graphics that state the correlations among maximum or central plate deflection, normal and shear stresses with the fiber angle, lamina number, and a/h ratio parameters.

The non-dimensional plate central deflection using the discretization of 4, 9, 16, and 25 elements show the result convergence in Figure 17.

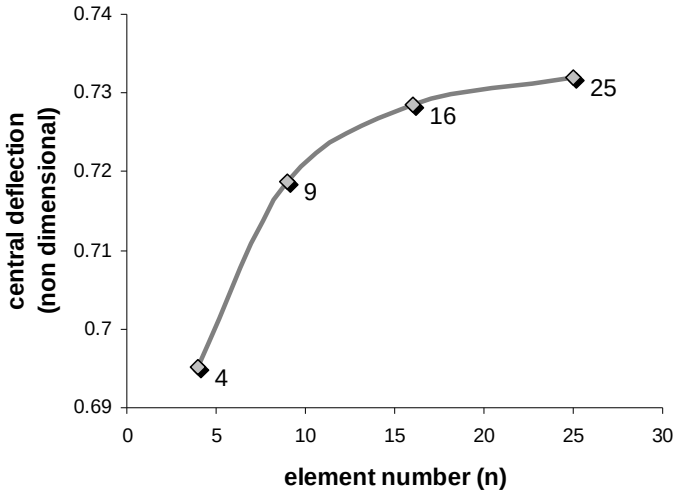

Figure 17. Element discretization number and plate central deflection relationship

Relative error percentage of HOLT model shown in Table 6:

Table 6. Deflection and relative error in HOLT model

Element number	Deflection w*	Relative error (%)
4	0.6951	6.497175141
9	0.7187	3.322571967
16	0.7286	1.990852838
25	0.7320	1.533494754
Exact elasticity theory	0.7343	0

For the sake of efficiency 16 element discretizations were used because they have adequate accuracy. The discretizations more than 16 elements will be costly in computer memory and time.

4.4. Discussion

4.4.1. Maximum Deflection

The central plate maximum deflection found by three models shown in Figure 18. The larger plate length dimension *a* the larger the deflection value *w* (dimensional), but non-dimensional value of deflection w* in Equation (33) get smaller in Figure 18. The maximum deflection in HOLT model approximate the exact results found from elasticity theory in all a/h ratio. The larger a/h ratio then three models coincide the results as shown in Figure 18. Otherwise, at the small a/h ratio, the deflection HOLT model and FOLT model differ significantly as shown in Figure 19. Figure 20 shows the relationship between fiber angle in 2nd and 3rd plies using symmetric angle-ply arrangement [0°/β°/β°/0°] and central deflection with varying a/h ratio.

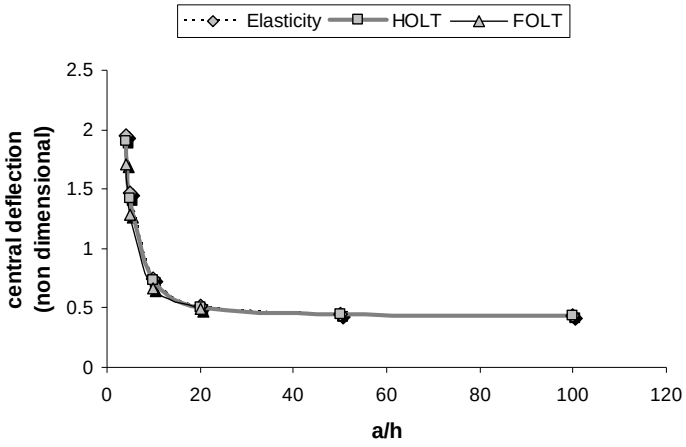

Figure 18. The relationship between a/h ratio and central deflection for three models

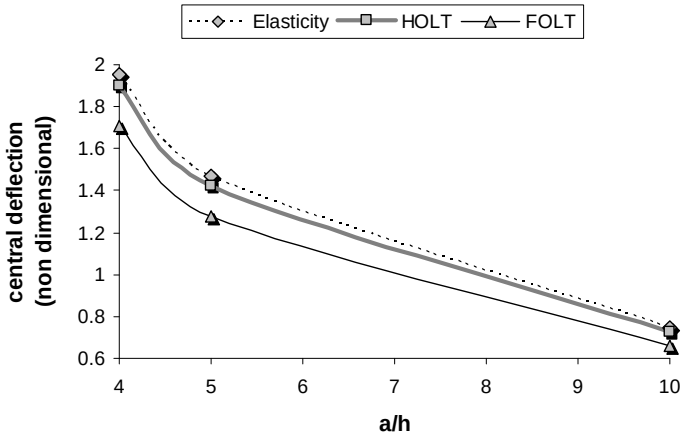

Figure 19. The difference of the deflection w* get significant at interval ratio of a/h=4 to a/h=10

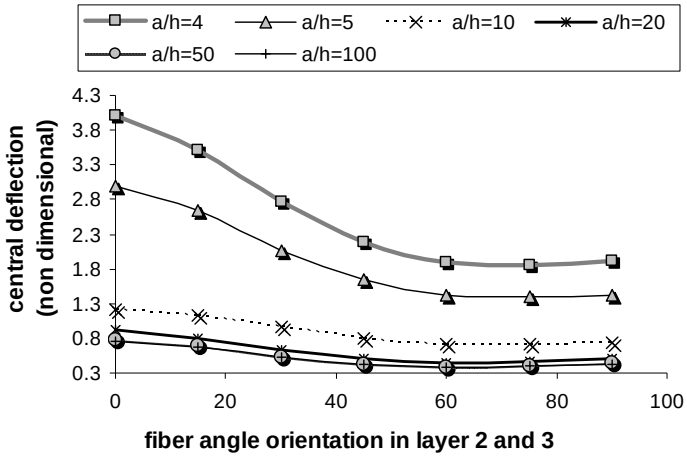

Figure 20. Fiber angle and non-dimensional central deflection relationship of 2nd and 3rd plies with varying a/h ratio

It can be seen on Figure 20 that deflection gets smaller if orthotropic fiber angle has perpendicular angle toward each other $\beta=0°$ or $\beta=90°$ or cross-ply laminate arrangement and vice versa, the deflection gets larger at the fiber angle ranged $0°<\beta<90°$ or angle-ply laminate configuration.

4.4.2. Stresses

Stress results from HOLT model agree well with Pagano's exact result derived from elasticity theory. FOLT model suffer inaccuracy at the small a/h ratio. However at the large a/h all models have coincided the results due to a small and negligible shear deformation in the thin plates case as shown and described in Figure 21 for principal normal stress in 1 direction.

The interlaminar principal normal and shear stresses distribution through the thickness for a symmetric cross-ply [0°/90°/90°/0°] arrangement using layer number n=4 in one of the loading case is shown in Figure 22 to Figure 26.

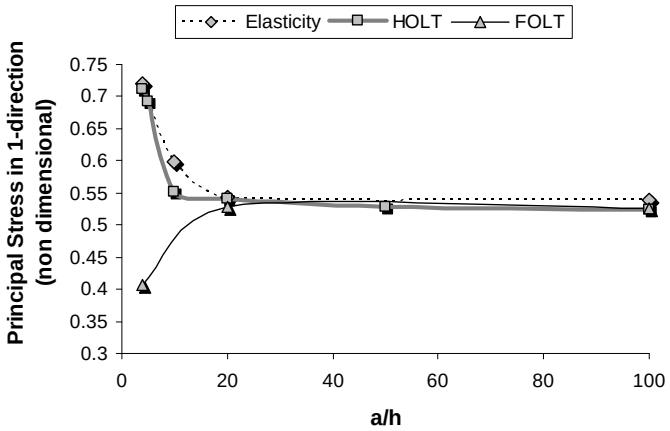

Figure 21. The a/h ratio and σ_1 relationship at x=a/2, y=b/2 and z= h/2 for three models

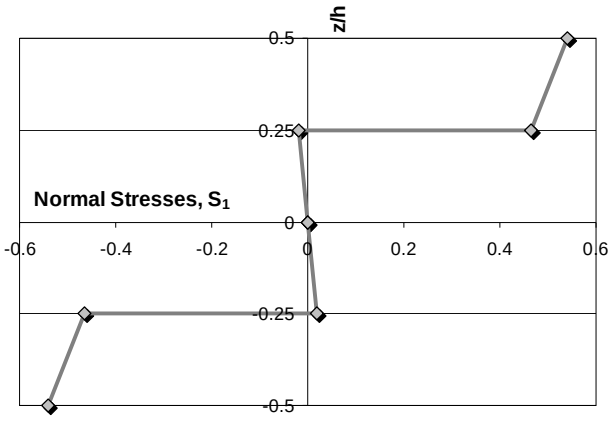

Figure 22. Principal Stress σ_1 ($^a/_2$,$^b/_2$,z) for n=4 layers $[0°/90°]_s$

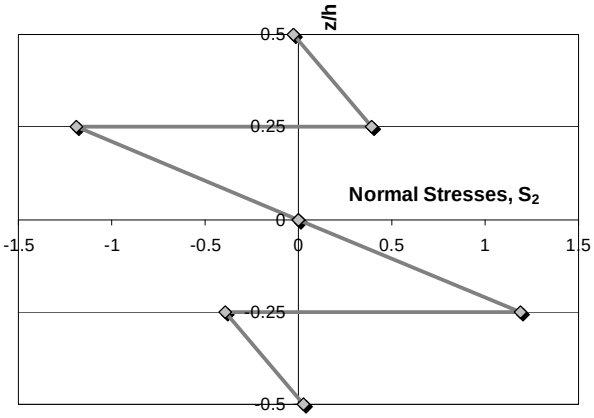

Figure 23. Principal Stress σ_2 ($^a/_2$,$^b/_2$,z) for n=4 layers $[0°/90°]_s$

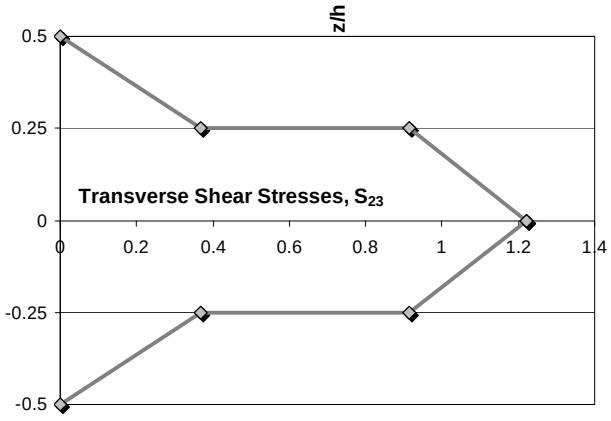

Figure 24. Transverse shear stress τ_{23} ($^a/_2$,$^b/_2$,z) for n= 4 layers $[0°/90°]_s$

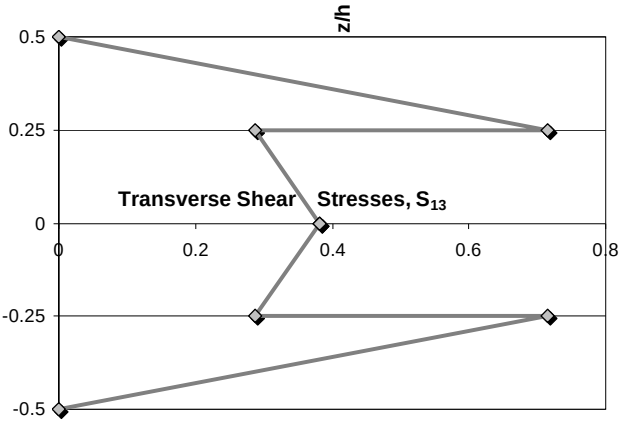

Figure 25. Transverse shear stress τ_{13} ($^{a}/_{2}$,$^{b}/_{2}$,z) for n= 4 layers $[0°/90°]_s$

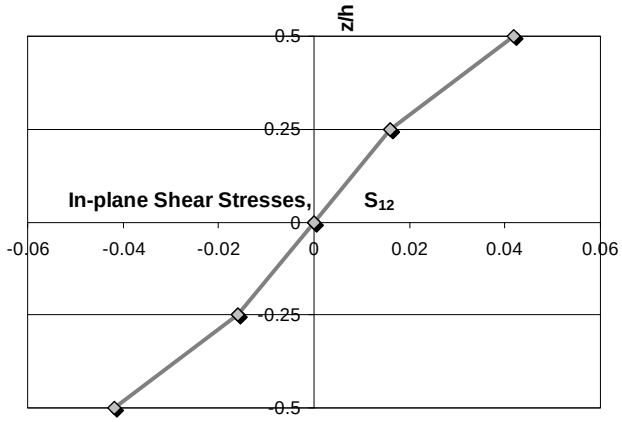

Figure 26. Principal shear stress τ_{12} ($^{a}/_{2}$,$^{b}/_{2}$,z) for n= 4 layers $[0°/90°]_s$

In the same structural dimension, stress patterns will vary and depend on the depth of point position, lamina number, fiber angle of each lamina, thickness and the heterogenity properties each lamina.

5. Conclusions

Regarding these studies it can be concluded that:

1. The deflection, normal and shear stresses in the bending part of present Liu-modified shell element in the HOLT model especially in rectangular laminated composite plates, have larger results compared with FOLT model at the small a/h ratio and almost the same at a/h ratio larger than 10.

2. The plate will be stiffer and or the deflection smaller if a symmetric cross-ply laminates (fiber angle 0° and 90° arrangement) is used.

3. The interlaminar stresses through the thickness is not distributed continuously, but they have certain patterns depending on depth of the point observed, lamina number, fiber angle of each layer, thickness and their heterogenity material properties, and a/h ratio.

The point can be suggested is that using higher order Gauss quadrature will reduce running analysis time without any refined elements required and without any harm to accuracy. It must be considered that using another lamination theory such as layerwise and zigzag theory – while keeping procedure efficient– so symmetric, odd and even lamina number inaccuracy can be avoided. Any other type of elements should be compared in both aspect of efficiency and accuracy like a solid shell element that they do not suffer any locking. Further research still needed to observe the temperature, dynamics, impacts, delamination, crack, buckling and postbuckling or a combination of them. Do they have a consistent result at all composite materials? None of shell elements pass both numerical and experimental tests as well.

References

Chia, C.Y. (1990), "Nonlinear Analysis of Plates", *Mc Graw Hill Inc.*, New York, NY., USA.

Cook, R.D. (1981), "Konsep dan Aplikasi Metode Elemen Hingga", *Terj: Bambang. Eresco*, Bandung.

Gibson, R. (1994), "Principles of Composite Material Mechanics", *Mc Graw Hill Inc*., New York, NY., USA.

Hull, D. (1981), "An Introduction to Composite Material", *Cambridge University Press.*, New York, NY., USA.

Ji, F.H. (1994), "A refined shear deformation theory of bending of isotropic plates", *Journal of Mechanics Structure and Machines*, Vol. 22, No. 4, Pages 397-427.

Kriz, R. (2000), « Microstructure Lectures", http://www.jwave.vt.edu/crcd/kriz/lectures/lect.html

Levinson, M. (1980), "An accurate simple theory of statics and dinamics of elastic plates", *Mechanics Research Communication*, Vol. 7, No. 6, Pages 343-350.

Liu, I., W. and Lin, C.C. (1994), "A new conforming plate bending element for the analysis of composite laminates", *Proceeding of National Science Council, ROC(A)*, Vol. 18, No. 6, Pages 561-569.

Reddy, J.N. (1984), "Energy and Variational Methods in Applied Mechanics with An Introduction to The Finite Element Methods", *John Willey & Sons*, Ottawa, ON., Canada.

Rochman, T. (2002), "Analisis pelat persegi berlapis model levinson dari bahan komposit dengan menggunakan metode elemen hingga", *Thesis*, Pascasarjana, Universitas Brawijaya, Malang, Indonesia.

Santoso, E.S. (1997), "Analisis Pelat Persegi Model Reissner-Mindlin dari Bahan Komposit Satu Arah dengan Sudut Ortotropi Menggunakan Metode Elemen Hingga", *Skripsi*. Fakultas Teknik, Universitas Brawijaya, Malang, Indonesia.

Venkateswara and Singh, G.D.R. (1995), "A discussion on simple third order theories and elasticity approaches for flexure of laminated plates", *Journal of Structural Engineering and Mechanics*, Vol. 3, No. 2, Pages 121-133.

Szilard, R. (1974), "Theories and Applications of Plate Analysis: Classical Numerical And Engineering Methods", *Wiley-VCH Verlag GmbH & Co*., Boschstr, Germany.

Timoshenko, S. and Woinowsky-Krieger, S. (1959), "Theory of Plates and Shells", 2nd Edition, *McGraw Hill*, New York, NY., USA.

Bert, W.C. (1984), "A critical evaluastion of new plate theories applied to laminated composites", *Journal of Composite Structure*, Vol. 2, Pages 315-328.

Weaver, W. and Johnson, P.R. (1984), "Finite Elements for Structural Analysis", *Prentice-Hall*, Englewood Cliffs., NJ., USA.